Nano Science and Nano Technology

An Indian Journal

Trade Science Inc.

Full Paper

Chemical reaction and crystalline procedure of bismuth titanate nanoparticles derived by metalorganic decomposition technique

W.L.Liu[1]*, X.Q.Wang[2], D.Tian[1], C.L.Xiao[1], Z.J.Wei[1], S.H.Chen[1]

[1]Provincial Key Laboratory of Glass and Ceramics, School of Materials Science and Engineering, Shandong Institute of Light Industry, Jinan, 250353, (P.R.CHINA)
[2]State Key Laboratory of Crystal Materials, Shandong University, Jinan, 250100, (P.R.CHINA)
E-mail : wlliu@sdu.edu.cn; liuwl@sdili.edu.cn

ABSTRACT

The homogeneous bismuth titanate single-phase nanoscaled ceramic powders have been prepared by means of metalorganic decomposition. The thermal decomposition/oxidation of the pre-heated precursor, as investigated by differential thermalgravimetric analysis, X-ray powder diffraction, and environment scanning electron microscope, lead to the formation of a well-defined orthorhombic bismuth titanate compound. Formation of the layered perovskite-like bismuth titanate occurs via intermediates with sequential changes in the coordination polyhedron of bismuth. The chemical reactions of precursor powder in heat treatment process have been investigated further by Raman and Fourier transform infrared spectra, and the reaction mechanism was tentatively proposed thereafter.

© 2010 Trade Science Inc. - INDIA

INTRODUCTION

Bismuth titanate ($Bi_4Ti_3O_{12}$, BTO) belongs to the family of ferroelectric materials with layered structures, which can be written as a general formula of $(Bi_2O_2)^{2+}(Bi_2Ti_3O_{10})^{2-}$. The layered structure is constructed by alternative stacking of a triple layer of TiO_6 octahedra (perovskite slab) and a monolayer of $(Bi_2O_2)^{2+}$ along the *c*-axis. Single crystal BTO has low dielectric permittivity and a very high Curie temperature ($T_c = 675°C$), which makes it useful for various applications such as memory elements, optical displays, and piezoelectric converters of pyroelectric devices in a wide temperature range from 20 to 600°C. BTO ceramics have been used in capacitors, transducers, sen-

sors, etc.[1,2]. The tuning of electric properties by compositional modification as well as the size effect can meet commercial specifications for Curie temperature, conductivity, coercivity, compliance, etc.[3,4].

Although BTO is normally prepared by solid-state reaction of Bi_2O_3 and TiO_2 at elevated temperatures up to 1100°C[5], owing to some inherent limitations of the process that yields large grain size of product phase, several alternate chemical syntheses routes have been proposed. These include coprecipitation, sol-gel, hydrothermal and molten salt synthesis[6-9]. Metalorganic decomposition (MOD) employed in the study offers the advantages of low calcining temperature, simplifying process, better homogeneity, stoichiometric composition control, and low cost. The formation mecha-

Full Paper

nism of the BTO prepared using MOD method, therefore, was proposed in order to get better understanding of the reaction process.

EXPERIMENTAL

The required amounts of bismuth nitrate [$Bi(NO_3)_3.5H_2O$] was dissolved in glacial acetic acid (CH_3COOH) by stirring at 60°C up to achieve complete dissolution. Stoichiometric tetrabutyl titanate [$Ti(OC_4H_9)_4$] was slowly dropped into the above solution under constant rate stirring. Acetylacetone ($CH_3COCH_2COCH_3$) as reagent was used to stabilize tetrabutyl titanate. And the solution was diluted with 2-methoxyethanol ($CH_3OCH_2CH_2OH$) to adjust viscosity and surface tension. The resultant solution was stirred at room temperature for 1 h and filtered whereafter to form the stock solution, which was yellow, clear, and transparent.

The precursor solution thus obtained was dried in an oven at 90°C for 10 h, resulting in the formation of a fine yellowish powder. After ground in an agate, the powder was annealed at various temperatures between 450 and 750°C. Thermal reactions taking place during the calcinations of the powder were analyzed in air by thermo-gravimetric and differential thermal analysis (TG/DTA, Netzsch STA 449c). The existing phases in the calcined samples were studied by X-Ray diffraction (XRD, Rigaku D/MAX-γA). Crystallite size of calcined powders was determined by X-ray line broadening using the Scherrer equation[10]. The evolution of the powder morphology with the calcination temperature was studied by an environment scanning electron microscope (ESEM, Quanta 200). The Raman measurements were performed in the backscattering geometry using a Ventuno21 NRS-1000DT instrument at room temperature to study the lattice dynamics and structural variety. The infrared (IR) spectra were measured from 400-4000cm^{-1} with a Bruker Tensor 27 FT-IR spectrometer to monitor the chemical reaction.

RESULTS AND DISCUSSION

Thermal analysis

The relative weight loss (44%) and differential thermal analysis of the pre-heated precursor, as shown in figure 1, indicate that heat begins to evolve at about 300°C and the second weight loss occurs around 600°C. It is seen from the curve of the DTA in this figure that two exothermic effects appear at about 350 and 750°C, respectively. Combined with TGA data, it is obvious that the endothermic effect at about 350°C is due to the decomposition and decarbonization of organic and inorganic compounds. It also demonstrates that the weight loss takes place in the endothermic processing between 270 and 420°C, which is about 24%. The DTA curve shows the exothermic effect at about 350°C, which probably also corresponds to the first nucleation events and the solid-state reaction, and it will be discussed in XRD data. With an increase in temperature, the second exothermic effect, which appears to be located at ~750°C is also present. Although no previous thermodynamic data have been found in the literature, the second exothermic effect may be attributed to the formation of small agglomerate of pure BTO ceramic powders, and the crystallization process of BTO is completed before 750°C. At that temperature the weight loss is finished. The crystallization process takes place simultaneously with the combustion of residual organic products and/or carbon.

XRD study

Diffraction is an appropriate technique when following the formation of a crystalline solid to obtain qualitative information about the course of a reaction and phase identification at each step. This information is the first step in being able to postulate reaction mechanisms.

The X-ray diffraction studies on the samples calcined at different temperatures for 5 min are shown in figure 2. The XRD pattern of initial powder confirms the amorphous nature, indicating that the powder is non-crystalline. The precursor shows evident crystallization as the temperatures increases to 450°C, and the three strong peaks correspond to $Bi_{12}TiO_{20}$ and $Bi_4Ti_3O_{12}$, respectively. In the short temperature interval of 450-550°C the precursor converts completely into the bismuth titanate compound (BTO and $Bi_{12}TiO_{20}$). Between 550 and 750°C all the amorphous phases react rapidly with the $Bi_{12}TiO_{20}$ intermediate phase leading to the formation of the BTO compound. It is also found from the XRD spectra that BTO powder has orthorhombic phase structure when the annealing temperature is 750°C. The
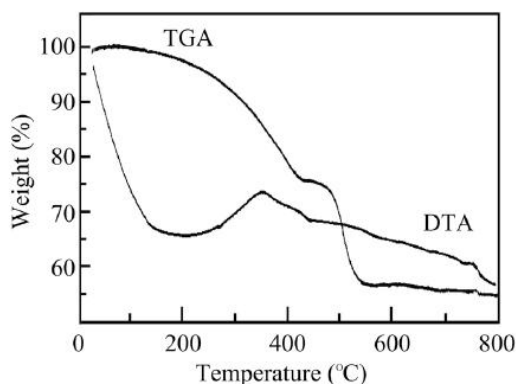
Figure 1 : TG/DTA curves for stock precursors

crystallite sizes of the powder heated at 750°C for 5 min are determined to be ~40nm from the half-width of the X-ray diffraction peaks using Scherrer's equation.

$$t = \frac{k\,\lambda}{\beta\cos\theta},$$

where θ is the diffraction angle, λ the average wavelength of X-ray, k the shape factor, and β is taken as half-maximum line breadth.

An increase in the grain size of BTO powder is observed as the annealing temperature increased up to 650°C but decrease remarkably thereafter. Figure 3 shows the ESEM micrographs of bismuth titanate nanoparticles at temperature of 750°C. The grain sizes estimated from SEM observations were different from those done by means of Schereer's equation. The Scherrer's equation assumes that all the crystallites are of the same size, but in an actual specimen, the size range and distribution affect β. Additionally, incoherent scattering from domains, distortions in the periodicity in the films, and micro-stress contribute to the line broadening and, hence, errors in the grain size estimation. Because the X-ray line broadening yields relative crystallite size, if absolute sizes are necessary then electron microscopy must be used to establish a basis for comparison.

Raman spectra

To further confirm the crystallization procedure of BTO in the MOD method, the powder precursors calcined at several temperatures were characterized using a Raman spectroscopy.

The Raman data on the powders calcined at 750°C shown in figure 4(e) agreed with the published results[11], even though it is not quite exact for the mode counting in polycrystalline material due to possible symmetry
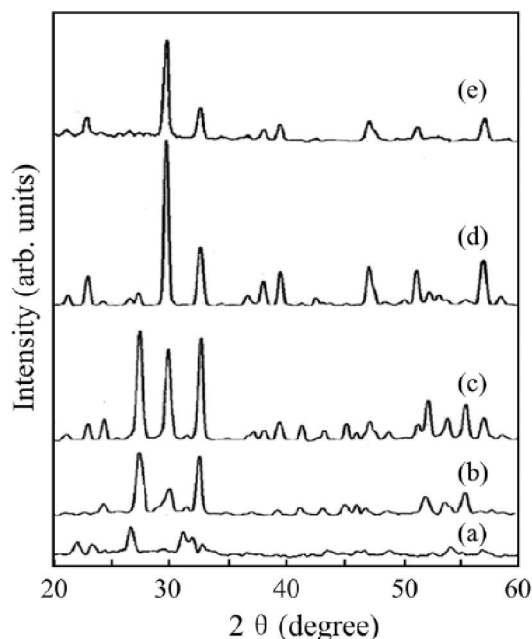

Figure 2 : X-ray diffraction patterns of BTO precursor calcined at various temperatures of 90 (a), 450 (b), 550 (c), 650 (d), and 750°C (e)

breaking, low peak intensity and overlap of vibration modes. In accordance with Raman data of $Bi_4Ti_3O_{12}$, $BaTiO_3$, and $PbTiO_3$[11-13], a shorter bond length of Ti-O than that of Bi-O, suggests that the Raman phonon modes of the corresponding higher wavenumbers, such as the modes at 610 and 847 cm^{-1}, originated mainly from the vibrations of atoms inside the TiO_6 octahedra. The peak at 847 cm^{-1} is attributed to the symmetric Ti-O stretching vibration, while the 610 cm^{-1} to asymmetric one; the 266 and 223cm^{-1} modes are ascribed to the O-Ti-O bending vibration. Although the mode at 223cm^{-1} is Raman inactive according to the O_h symmetry of TiO_6, it is often observed because of the distortion of octahedron. The mode at 326cm^{-1} is from a combination of the stretching and bending vibrations. The two modes at 533cm^{-1} and 564cm^{-1} correspond to the opposing excursions of the external apical oxygen atoms of the TiO_6 octahedra. The TiO_6 octahedra exhibit considerable distortion at room temperature so that some phonon modes e.g. at 326, 533, 610, and 847cm^{-1}, appear wide and weak, which are expected to induce ferroelectric anomaly of BTO. The Raman modes of the corresponding lower wavenumbers, such as the mode at 117cm^{-1}, originated mainly from the vibrations between Bi and O atoms, which can be confirmed by the shift to higher wavenumber due to the modification of a lighter Sm atom at a Bi site with in-
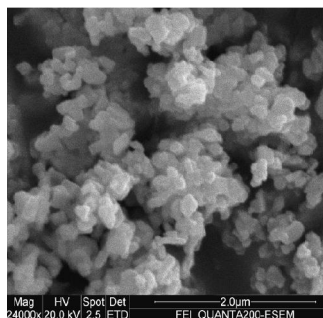
Full Paper

Figure 3 : ESEM micrographs of nanocrystalline BTO calcined at 750°C for 5min

creasing doping concentration[14,15].

In Raman spectra of powders calcined at 450-750°C for 5 min, figure 4, a few extra peaks or shoulders not identified with BTO were detected at 152, 319 and 538cm^{-1} at 450°C, and 158, 251, and 326cm^{-1} at 550°C. In the samples annealed at 650°C three broad peaks at 339, 501 and 635cm^{-1} were observed.

From the above results, the following can be pointed out. (a) The sharp increase in the intensity of the 265cm^{-1} band and the appearance of a band at 538cm^{-1} along with three other peaks at 152, 319 and 849cm^{-1} in the sample calcined at 450°C, indicated the rearrangement of a binary Bi_2O_3-TiO_2 intermediate structure before the formation of BTO phase[16,17]. Such a binary intermediate phase, according to the X-ray diffraction results, seems to correspond to the $Bi_{12}TiO_{20}$ compound, albeit this is not clearly established. The Raman spectra are in agreement with the data reported in the literature within the experimental errors[11]. The major lines associated to crystalline $Bi_{12}TiO_{20}$ were identified in the sample. However, it has to emphasize that the data from the literature was obtained from Raman scattering using single crystals, and the measurements were performed in powdered polycrystalline samples. This could explain the large bandwidth and minor frequency-shift of the optical lines associated to polycrystalline samples. (b) Although the spectrum for the sample heated at 550°C was similar to that after 650°C except for the almost disappearance of the bands at 538cm^{-1}, but the appearance of a band at 158 and a shoulder at 515 cm^{-1} indicated the coexistence of the two $Bi_{12}TiO_{20}$ and BTO phases, which is in agreement with the DTA and X-ray diffraction results. (c) The complete disappearance of all the Raman bands corresponding to the intermediate phase and, on the other hand, the increase in the intensity of the peaks at 266, 533 and 847cm^{-1}, which are

representative of a typical mixed-layered perovskite structure[17], indicated the formation of a not well crystallized BTO ternary phase close to the $Bi_4Ti_3O_{12}$ composition.

From the above results, we can suggest that, in a first step, the formation of $Bi_{12}TiO_{20}$ particles might be consistent with an Avrami-type nucleation and growth mechanism[18], in which the particles continuously nucleated three-dimensionally within the amorphous polymeric precursor matrix below 550°C. After the nucleus of crystal appears, the primary particle size gradually increases from the randomly distributed nuclei with the increasing temperature. The amount of the intermediate $Bi_{12}TiO_{20}$ phase rapidly decreased with the BTO formation and, finally, crystal growth of BTO by a solid-state reaction as the heat-treatment temperature increased takes place.

FTIR measurements

The IR spectra of the initial and post-annealed powders of BTO are shown in figure 5. After drying at 90°C, the spectrum is complex due to the existence of lots of organic compounds. Band at 3500~3200cm^{-1} is a characteristic group frequency from the stretch vibration of -OH[19]. The stretch -CH_2 of located at 2930cm^{-1}. The broad band around 1750cm^{-1} comes from C=O stretch vibration. The peaks of 1385, 1024, and 731cm^{-1} are the characteristic ones of NO_3^- group. The band at 1285 cm^{-1} can be assigned to bending/stretching vibrations of -COOH. The band at 1100 cm^{-1} is the stretching mode of C–O group, and the broad one around 700~400cm^{-1} originates from the metal-oxygen (M-O) vibration. After annealing at 450°C, many vibration lines disappear because of the evaporation of most solvents and decomposition of the organic ingredient. The strong and characteristic band of 1385cm^{-1} is from the nitrate group. The peak at 2336cm^{-1} is a characteristic pattern for the -COOH group. The only feature in spectra of 550, and 650°C heated powders is the band at around 600cm^{-1}, originating from M-O bonds. The IR results indicated that most decomposition could be achieved by heating above 650°C.

Reaction mechanism

In Bi-Ti solution system, $Ti(OC_4H_9)_4$ reacts easily with CH_3COOH to yield $Ti(OC_4H_9)_{4-x}(CH_3COO)_x$ that
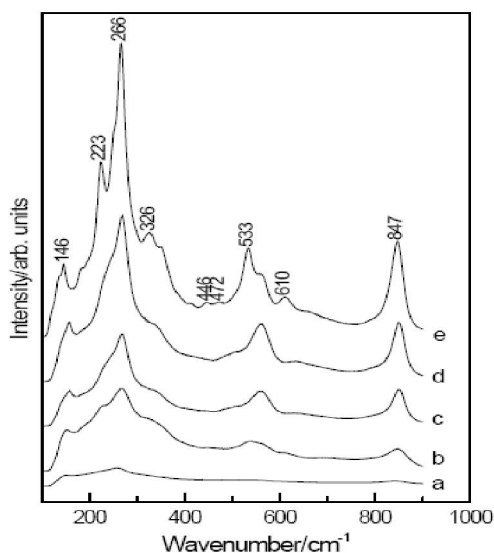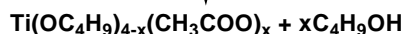
W.L.Liu et al.

Figure 4 : The evolution of the BTO Raman bands with temperature: (a) 90, (b) 450, (c) 550, (d) 650, and (e) 750°C

has a very slow hydrolysis rate in a strong acidity solution:

$$Ti(OC_4H_9)_4 + xCH_3COOH$$

$$\downarrow \tag{1}$$

$$Ti(OC_4H_9)_{4-x}(CH_3COO)_x + xC_4H_9OH$$

On the other hand, H^+ of acetic acid easily attacks alkoxy group ($-OC_4H_9$) of $Ti(OC_4H_9)_4$, which will expedite the hydrolysis reaction:
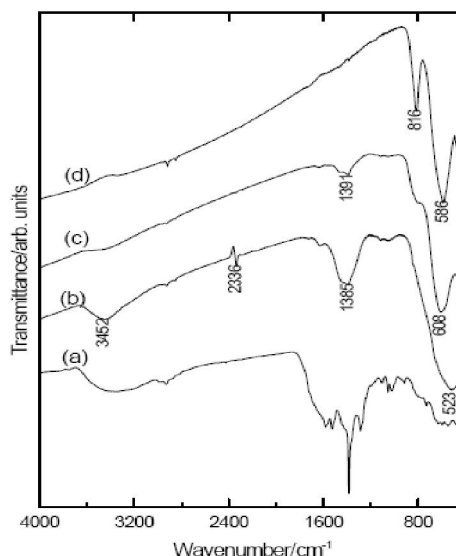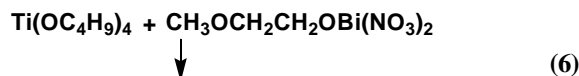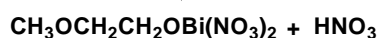
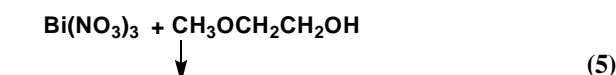$$\equiv Ti-OC_4H_9 + H^+ + H_2O$$

$$\downarrow$$

$$\equiv Ti-OH^+ C_4H_9 + H_2O \tag{2}$$

$$\downarrow$$

$$\equiv Ti-OH + C_4H_9OH + H^+$$

$$\equiv Ti-OH + \equiv Ti-OC_4H_9 \longrightarrow \equiv Ti-O-Ti \equiv \tag{3}$$

$$\equiv Ti-O-Ti \equiv + \equiv Ti-OH$$

$$\downarrow$$

$$\equiv Ti-O-Ti(OC_4H_9)_2-O-Ti \equiv \tag{4}$$

$$\downarrow$$

$$\equiv Ti-O-[Ti(OC_4H_9)_2]_n-O-Ti \equiv$$

$$Bi(NO_3)_3 + CH_3OCH_2CH_2OH$$

$$\downarrow \tag{5}$$

$$CH_3OCH_2CH_2OBi(NO_3)_2 + HNO_3$$

$$Ti(OC_4H_9)_4 + CH_3OCH_2CH_2OBi(NO_3)_2$$

$$\downarrow \tag{6}$$
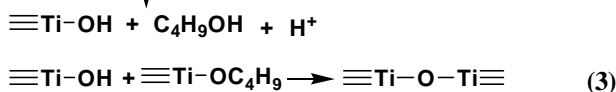
$$Ti(OC_4H_9)_3OCH_2CH_2OBi(NO_3)_2 + C_4H_9OCH_3$$
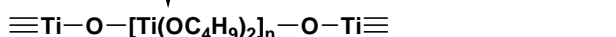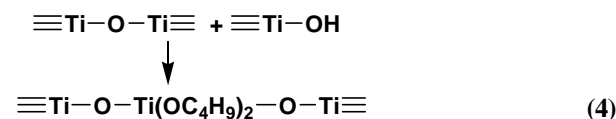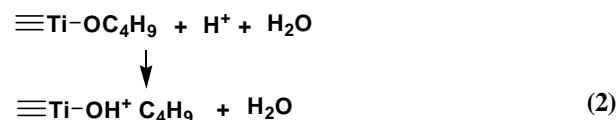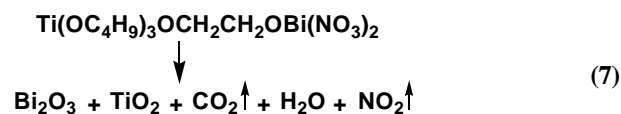

Figure 5 : FTIR spectra of BTO precursor post-annealed at temperatures of 90 (a), 550 (b), 650 (c), and 750°C (d) for 5 min

According to the above-mentioned analyses and the experimental results, the following reaction scheme is the most reasonable to describe the decomposition process:

$$Ti(OC_4H_9)_3OCH_2CH_2OBi(NO_3)_2$$

$$\downarrow \tag{7}$$

$$Bi_2O_3 + TiO_2 + CO_2\uparrow + H_2O + NO_2\uparrow$$

Bismuth titanate $Bi_{12}TiO_{20}$ is crystallochemically related to γ-Bi_2O_3; these compounds have similar structural frameworks and almost identical cubic cell parameters[20]. In view of this fact, formation of $Bi_{12}TiO_{20}$ in the Bi_2O_3-TiO_2 system can be considered as a phase transition from α-Bi_2O_3 to γ-Bi_2O_3 initiated by incorporation of a titanium dioxide admixture into the Bi_2O_3 structure.

The solid-phase synthesis of $Bi_4Ti_3O_{12}$ involves occurrence of both rearrangement and transport processes; thus, formation of $Bi_4Ti_3O_{12}$ occurs by the mechanism of successive rearrangements:

$$Bi_2O_3 + TiO_2 \longrightarrow Bi_{12}TiO_{20} \tag{8}$$

$$Bi_{12}TiO_{20} + TiO_2 \longrightarrow Bi_4Ti_3O_{12} \tag{9}$$
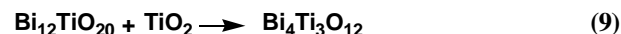
This transformation pattern reflects the crystallochemical genesis of the structure in the course of the solid-phase reaction. The structure formation involves a successive increase in the number of the nearest atoms adjacent to Bi, with the last, high-temperature stage being accompanied by a considerably larger change in the bismuth coordination number than the first,

Full Paper

low-temperature stage[20].

CONCLUSIONS

In summary, homogeneous and fine BTO ceramic powders have been prepared by metalorgainc decomposition method. Based on TGA/DTA, and XRD results, we conclude that the synthesis of the BTO compound takes place through the formation of an intermediate phase of composition $Bi_{12}TiO_{20}$, which is formed during the heating between 350 and 550°C. Prolonged heat treatment between 550 and 750°C promote a rapid consumption by solid-state reaction of the intermediate phase with the formation of BTO, without any indication on the formation of other different phases or segregation of the individual metal oxides. These results support the contention for the metalorganic precursor synthesis method as useful to prepare ceramics with complex composition such as those of bismuth titanates. The postulated mechanisms are further confirmed due to the structural variety as shown in Raman and FTIR studies.

ACKNOWLEDGEMENT

REFERENCES

[1] T.Takenaka, K.Sakata; J.Appl.Phys., **55**, 1092 **(1984)**.
[2] A.Fouskova, L.E.Cross; J.Appl.Phys., **41**, 2834 **(1970)**.
[3] O.Alvarez-Fregoso; J.Appl.Phys., **81**, 1378 **(1997)**.
[4] T.Takenaka, K.Sakata; Ferroelectrics, **38**, 769 **(1981)**.
[5] Y.Yoneda, J.Mizuki; Appl.Phys.Lett., **83**, 275 **(2003)**.
[6] A.Q.Jiang, G.H.Li, L.D.Zhang; J.Appl.Phys., **83**, 4878 **(1998)**.
[7] H.S.Gu, A.X.Kuang, X.J.Li; Ferroelectrics, **211**, 271 **(1998)**.
[8] Q.Yang, Y.Li, Q.Yin, P.Wang, Y.B.Cheng; J.Euro. Ceram.Soc., **23**, 161 **(2003)**.
[9] T.Kimura, T.Yamaguchi; Ceram.Int., **9**, 13 **(1983)**.
[10] K.P.Klug, L.E.Alexander; 'X-Ray Diffraction Procedures', John Wiley & Sons, New York, **(1974)**.
[11] H.Idink, V.Srikanth, W.B.White, E.C.Subbarao; J.Appl.Phys., **76**, 1819 **(1994)**.
[12] P.R.Graves, G.Hua, S.Myhra, J.G.Thompson; J.Solid State Chem., **114**, 112 **(1995)**.
[13] P.S.Dobal, R.S.Katiyar; J.Raman Spectrosc., **33**, 405 **(2002)**.
[14] W.L.Liu, H.R.Xia, H.Han, X.Q.Wang; J.Crystal Growth, **264**, 351 **(2004)**.
[15] W.L.Liu, H.R.Xia, H.Han, X.Q.Wang; J.Solid State Chem., **177**, 3021 **(2004)**.
[16] J.Meng, G.Zou, Y.Zhao, Q.Cui, D.Li; Physics Letters, A., **163**, 135 **(1992)**.
[17] J.Meng, R.S.Katiyar, G.T.Zou; J.Raman Spectrosc., **28**, 797 **(1997)**.
[18] M.Avrami; J.Chem.Phys., **8**, 1103 **(1939)**; M.Avrami; J.Chem.Phys., **8**, 212 **(1940)**, M.Avrami; J.Chem.Phys., **9**, 177 **(1941)**.
[19] X.Jing, S.Chen, E.Yao; Introduction of IR Spectra, Tianjian Technology Press, Tianjin, **(1992)**.
[20] M.I.Morozov, L.P.Mezentseva, V.V.Gusarov; Russian Journal of General Chemistry, **72**, 1038 **(2002)**.